

1 **Quantitative evaluation of the non-thermal effect in microwave induced polymer**
2 **curing**

3 Li Kun¹, Ping Tuo², Zhang Haobo¹, Zhang Junying¹, Cheng Jue^{1*}, Gao Feng^{1*}

4 1. Key Laboratory of Carbon Fiber and Functional Polymers, Ministry of Education, Beijing University
5 of Chemical Technology, Beijing 100029, P.R. China.

6 2. Beijing Spacecrafts, China Academy of Space Technology, Beijing 100194

7

8 *Corresponding author: Dr. Gao Feng & Prof. Cheng Jue

9 Tel: +86-10-64425439; E-mail: gaofeng@mail.buct.edu.cn (Gao. F); chengjue@mail.buct.edu.cn
10 (Cheng. J).

11 **Supplementary section**

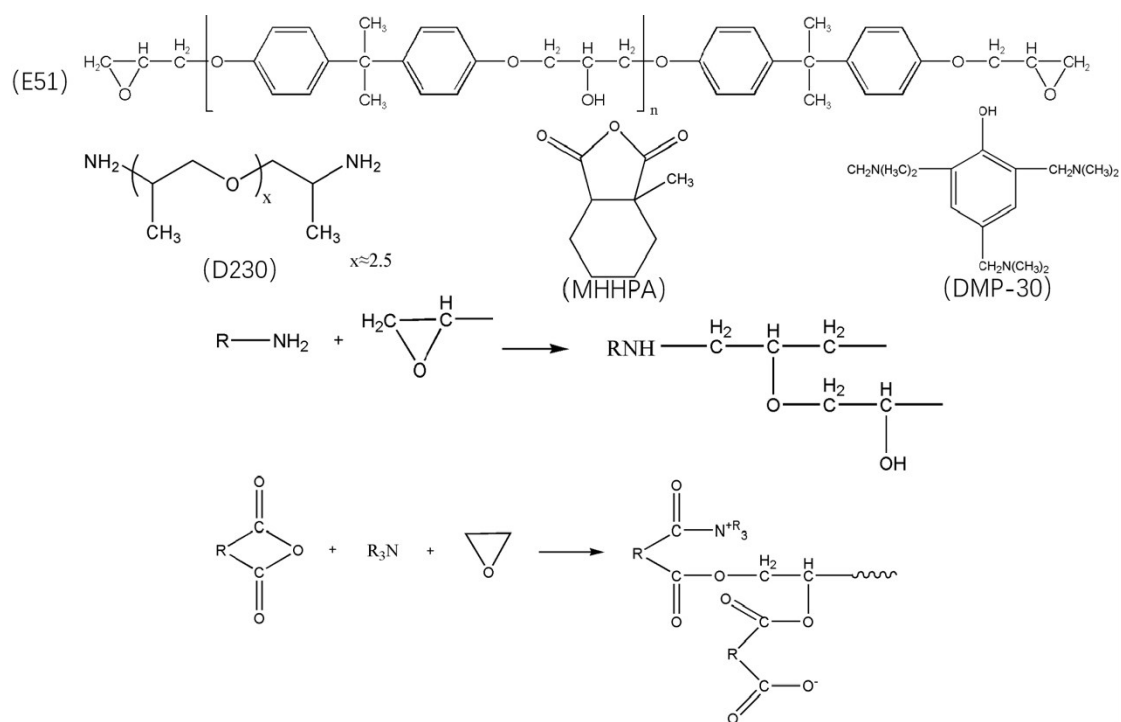
12 1. Material

13 2. Non-Isothermal and Isothermal curing reaction kinetics supplementary
14 date

15 3. Isothermal microwave curing reactor parameter

16

17



1

2 **Fig. S1. The curing process of the matrix resin used in this experiment.**

3

4 During the experiment, the temperature in the oil bath and microwave reactor after
 5 the device was circulated for 15 minutes were tested at different temperatures condition
 6 (Table S1).

7 **Table S1. Temperature on both sides of the microwave reactor.**

Circulation time/min	Oil bath temperature/°C	Microwave reactor temperature/°C
15	89	90
15	150	150
15	180	180

8 The data indicated that the temperature of the oil bath was basically the same as
 9 the microwave reactor, that was, the temperature of the system can be accurately

1 controlled by controlling the temperature of the oil bath and the silicone oil circulation.

2

3 **Table S2. Microwave induced isothermal resin reactor performance parameter.**

Parameter	
Power supply	AC 220V±10% 50Hz
Input power	1350W
Microwave power	≤900W(0-900 Continuous automatic frequency conversion adjustment)
Microwave frequency	2450MHz±50Hz
temperature control	Constant temperature mode (Room temperature-250°C)
Resolution	0.1 °C
Temperature control accuracy	±0.1 °C
Work time	Unlimited duration
Work size	325*325*202 (Length* height *width) mm
Dimensions	500*420*400 (Length* height *width) mm

4

5 The temperature difference between the sandwich structure and the silicone oil
6 was calculated according to the heat conduction Eq. (S1).

$$Q = \frac{T_1 - T_2}{\frac{b}{\lambda_m A}} \quad (S1)$$

Where Q is the energy power through KBr on one side; T_1-T_2 is the temperature difference; b is the thickness of KBr sheet; A is the area of heat transfer; λ_m is the thermal conductivity of KBr. Since the epoxy resin sample was flimsy, the temperature of each part was the same, and the corresponding value in the above equation was taken into the calculation, $2Q$ is basically the same as the selected microwave irradiation power of 240 W. The results have shown that even if all the energy provided by microwave irradiation was absorbed by the sample, the temperature difference will not be greater than 1K, and the heat generated during the reaction can be quickly derived, thereby eliminating the effect of thermal effects on the reaction.

We did build the isothermal reactor in this work to peel off the thermal effect of the microwave irradiation which was described in the introduction part. The temperature of the ‘heating-while-cooling’ system was monitored by the fiber-optic probes and adjusted by turning the external cooling liquid temperature, the non-thermal effect of microwave was able to be evaluated under this isothermal reaction condition. Silicone oil was chosen as the cooling fluid to stabilize the temperature of the resin due to its low dielectric constant. Thus, the microwave hardly affected the temperature of the cooling fluid. The influence of reaction temperature towards the reaction kinetic was minimized as much as possible, and the influence of hardener structure and the reaction temperature under microwave irradiation was evaluated.

The temperature of the ‘heating-while-cooling’ system was monitored by the fiber-optic probes, and the temperature difference will not be greater than 0.5K.

Table S3. Reaction temperature setting.

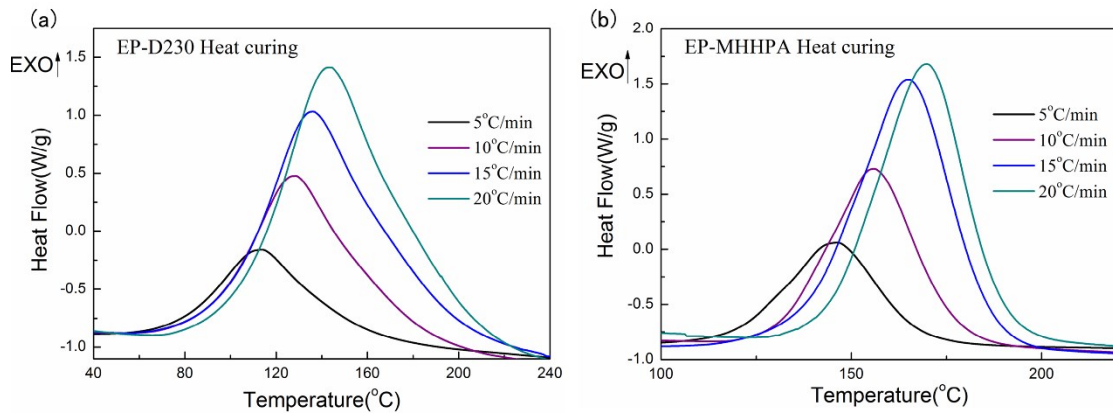
Thermostatic microwave reactor/°C	Oven temperature/°C
50.0	51.1

55.0	56.1
60.0	61.1
65.0	66.2
70.0	71.2
75.0	76.1
80.0	81.2
85.0	86.1
110.0	111.3
115.0	116.2
120.0	121.3
125.0	126.3

1 The reaction temperature of the samples without microwave irradiation was
2 corrected and the reaction temperature in the oven has been raised to ensure that the
3 resin is at the same curing temperature, in order to study scientifically the non-thermal
4 effect of the accelerated reaction mechanism of microwave curing.

5

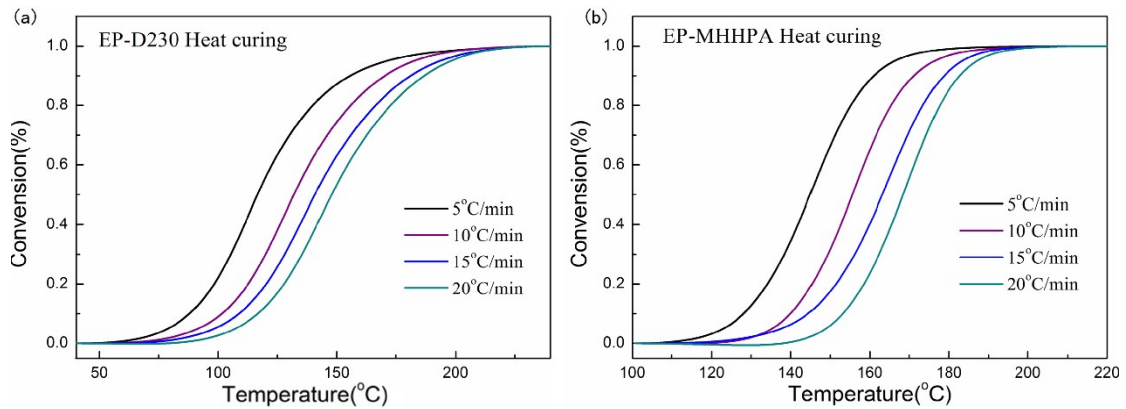
6 **Calculation of Non-Isothermal Curing Reaction Kinetics**



1

2 **Fig. S2. DSC thermographs of (a) EP-D230, (b)EP-MHHPA at the heating rates of 5, 10, 15, and**
 3 **20 °C/min, respectively.**

4 The model free advanced iso-conversion kinetic analysis was used to investigate
 5 the reactions [1-4]. The data of non-isothermal DSC curing reaction of EP-D230 and
 6 EP-MHHPA systems was presented by Fig. S2. The initial curing temperature (T_i), peak
 7 temperature (T_p), and finishing temperature (T_f) increase continuously for all the
 8 samples with the increasing of the heating rate, and the curing time decreases during
 9 this process. It was assumed that all the exothermic reaction was directly proportional
 10 to the fractional conversion.



11

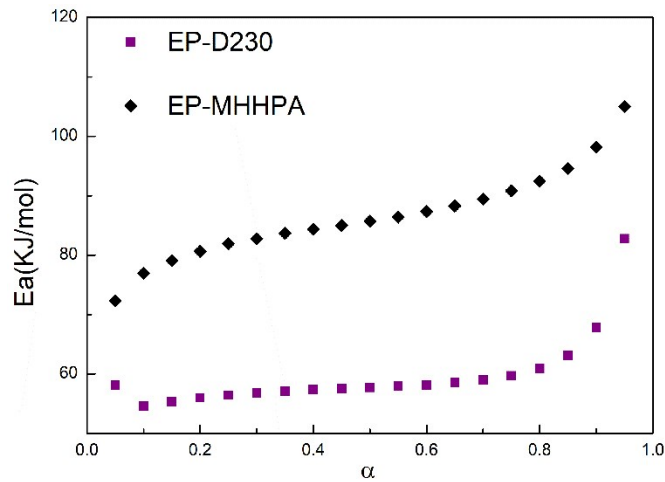
12 **Fig. S3. Conversion α as a function of temperature at different heating rates :(a), EP-D230;(b) EP-**
 13 **MHHPA.**

14 The temperature-dependent reaction rate fractional conversion and the
 15 temperature-dependent reaction rate constant ($k(T)$) were calculated by Arrhenius
 16 equation [5]. Curing reaction rate of epoxy resin systems was calculated by Eq. (1):

$$\frac{d\alpha}{dt} = \frac{1}{\Delta H_0} \frac{dH}{dt} = k(T)f(\alpha) = A \exp\left(\frac{-E_a}{RT}\right) f(\alpha) \quad (1)$$

Where t is the reaction time; ΔH_0 is the total reaction enthalpy; $\frac{dH}{dt}$ is the reaction heat flow rate; α is the fractional conversion; $\frac{d\alpha}{dt}$ is the reaction rate; T is the Kelvin degree; $f(\alpha)$ is a function representing the kinetic model; $k(T)$ is the temperature-dependent reaction rate constant; A is the pre-exponential factor; E_a is the activation energy; R is the universal gas constant.

Fig. S3 (a) and (b) show the dependence of the fractional conversion on the temperature for EP-D230, and EP-MHHPA systems with the heating rates climbing from 5 °C/min, 10 °C/min, 15 °C/min, to 20 °C/min.



10

11 **Fig. S4. Variation of effective activation energy with fractional conversion for EP-D230 and EP-**
 12 **MHHPA.**

13 Model-free advanced iso-conversion kinetic analysis developed by Vyazovkin is
 14 a powerful way to investigate activation energy, which is based on the iso-conversional
 15 principle [1-3,6]. It states that the reaction rate at constant extent of conversion is a
 16 function of the temperature which can be used reveal the relationship between the
 17 activation energy and the fractional conversion for thermosetting reactions without
 18 kinetic models [6]. In this work, Vyazovkin kinetic analysis method was used to
 19 estimate the variation of activation energy with fractional conversion for the curing
 20 reactions of EP-D230 and EP-MHHPA systems [1,6]. Generally, the analytic

1 expressions for this method can be expressed by Eq. (2) and (3):

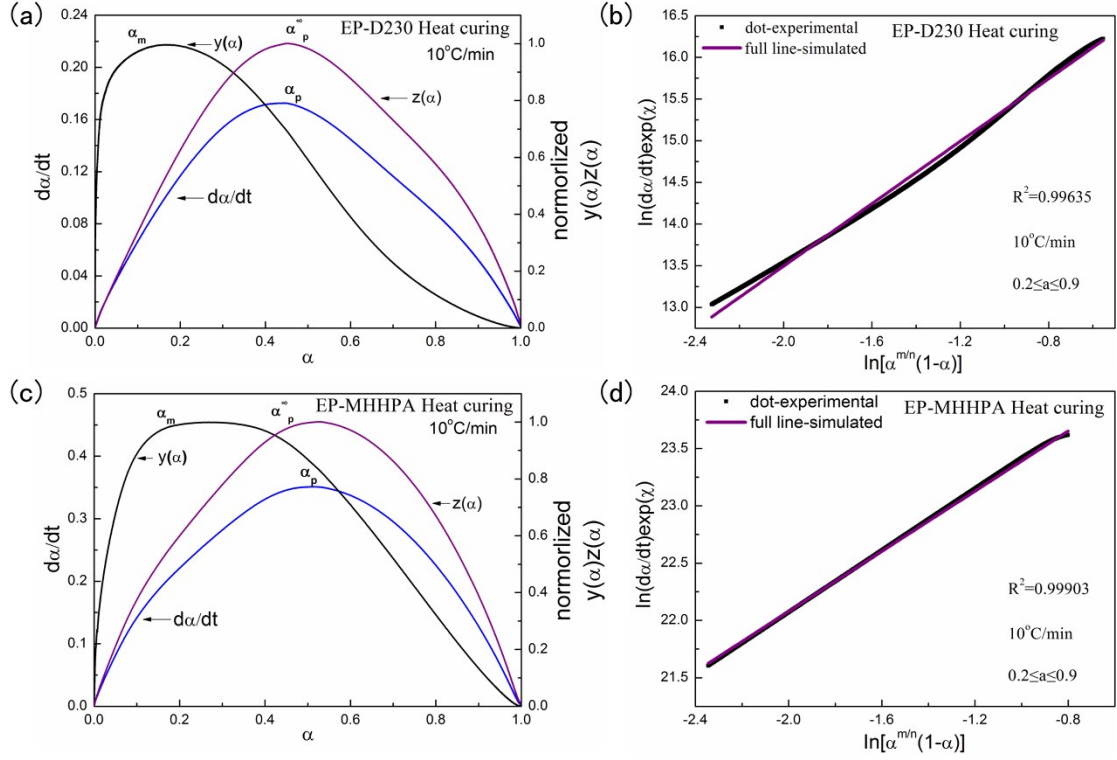
$$2 \quad \varphi(E_\alpha) = \sum_{i=1}^n \sum_{j \neq i}^n \frac{J[E_\alpha, T_{\alpha,i}] \beta_j}{J[E_\alpha, T_{\alpha,j}] \beta_i} = \min \quad (2)$$

$$3 \quad J[E_\alpha, T_\alpha] \equiv \int_0^{T_\alpha} \exp\left(\frac{-E_\alpha}{RT}\right) dt \quad (3)$$

4 Where subscripts (*i and j*) present the ordinal sequence of the thermal
5 measurements performed under different programs; *J* is the temperature integral. The
6 data of variation of activation energy with fractional conversion was presented by Fig.
7 S4. Nonlinear interpolation was used to determine the values of t_α in this work. The
8 small increment of fractional conversion, $\Delta\alpha$ (set as 0.05), and the temperature integral
9 were evaluated according to the trapezoid rule. To obtain the temperature integral value,
10 it was substituted in Eq. (2), and the minimization was carried out to find E_α . The same
11 α values are straight line and the slope can obtain the E_α value.

12 The E_α decreasing at the initial stage may be due to the controlling autocatalytic
13 mechanism. The value of α ranged from 0.2 to 0.6 with the E_α values remained
14 practically constant suggesting that the initial stage was dominated by a single reaction.
15 At the end of this stage, the chain mobility was restricted by the increasing molecular
16 weight leading to the climb up of the activation energy. The curing rate in the glassy
17 state decreased dramatically which relied on the diffusion of small and unreacted
18 groups remained in the matrix. Results indicated that the vitrification caused the
19 considerable decrease in the molecular mobility leading to the increase of the effective
20 activation energy with the increasing reaction extent [7,9,10].

21



1

2 **Fig. S5. Non-isothermal analysis of DGEBA without microwaves: (a) $d\alpha/dt$ versus the fractional**
 3 **conversion of EP-D230; (b) $[(d\alpha/dt) \exp(\chi)]$ versus $\ln[\alpha^m(1-\alpha)]$ of D230; (c) $d\alpha/dt$ versus the**
 4 **fractional conversion of EP-MHHPA; (d) $[(d\alpha/dt) \exp(\chi)]$ versus $\ln[\alpha^m(1-\alpha)]$ of EP-MHHPA.**

5 Málek [4,5] method was used to determine the appropriate kinetic model and the
 6 rate equation of curing reaction from $y(\alpha)$ and $z(\alpha)$:

7
$$y(\alpha) = \frac{d\alpha}{dt} \exp(\chi) \quad (4)$$

8
$$z(\alpha) = \pi(\chi) \frac{d\alpha T}{dt \beta} \quad (5)$$

9 Where χ is equal to the E_a/RT and $\pi(\chi)$ is the integration of the temperature.
 10 Furthermore, $\pi(\chi)$ can be calculated by Eq. (6) [8]:

11
$$\pi(\chi) = \frac{\chi^3 + 18\chi^2 + 88\chi + 96}{\chi^4 + 20\chi^3 + 120\chi^2 + 240\chi + 120} \quad (6)$$

12 The SB (m, n) [1,4,5] can be used to fit the non-isothermal curing kinetic of EP-
 13 D230 and EP-MHHPA systems (Eq.7) according to the judging standard of the Málek
 14 [1,4,5] method.

$$\ln\left[\frac{da}{dt}\exp(\chi)\right] = \ln A + n[\ln a^{\frac{m}{n}}(1-a)] \quad (7)$$

The reaction temperature was determined according to the non-isothermal analysis of matrix resin based on the Málek method for the better of the reaction kinetic equation [9,10].

Fig. S5.(a) and (c) show the variation of experimental reaction rate (da/dt), normalized $y(\alpha)$, and normalized $z(\alpha)$ versus the fractional conversion of EP-D230 and EP-MHHPA systems with the heating rate of 10 °C/min. Fig. 2(b) and (d) show the variation of $\ln[(da/dt) \exp(\chi)]$ versus $\ln[\alpha^{m/n}(1-\alpha)]$ for EP-D230 and EP-MHHPA systems with the heating rate of 10 °C/min. The apparent dynamic equations for the curing reactions of EP-D230 and EP-MHHPA systems can be obtained by substituting the calculated kinetic parameters in Table S4. It can be clearly observed that $0 < \alpha_M < \alpha_p^\infty$ and $\alpha_p^\infty \neq 0.632$ [6].

Table S4. The peak values of da/dt , $y(\alpha)$ and $z(\alpha)$, along with the calculated kinetic parameters.

Sample	β (°C/min)	α_M	α_p^∞	α_p	n	m	$\ln A$
D230	5	0.148	0.463	0.450	2.01	0.35	17.35
	10	0.185	0.453	0.442	1.87	0.38	17.24
	15	0.156	0.441	0.423	1.85	0.34	17.16
	20	0.172	0.449	0.434	2.00	0.41	17.61
Mean		0.165	0.451	0.437	1.93	0.37	17.34
MHHPA	5	0.266	0.555	0.542	1.34	0.49	24.61
	10	0.271	0.526	0.510	1.31	0.49	24.70
	15	0.243	0.579	0.558	1.10	0.35	24.33
	20	0.284	0.563	0.548	1.14	0.45	24.57
Mean		0.266	0.556	0.539	1.22	0.44	24.55

14

15 EP-D230:

$$\frac{d\alpha}{dt} = 3.39 \times 10^7 \exp\left(\frac{-58933}{RT}\right) \alpha^{0.37} (1-\alpha)^{1.93} \quad (8)$$

17 $\alpha \in [0, 1]$

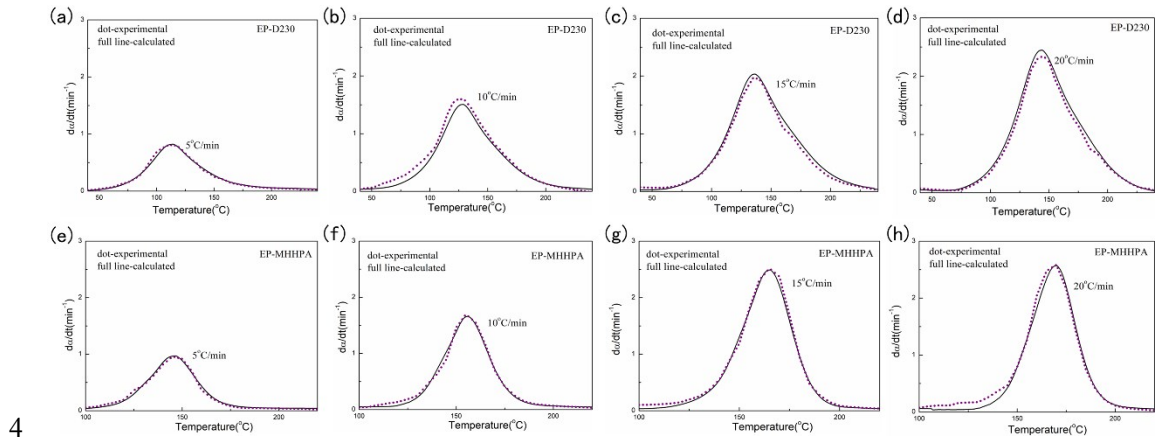
18 EP-MHHPA:

$$\frac{d\alpha}{dt} = 4.59 \times 10^{10} \exp\left(\frac{-87421}{RT}\right) \alpha^{0.44} (1-\alpha)^{1.22} \quad (9)$$

1 $\alpha \in [0, 1]$

2

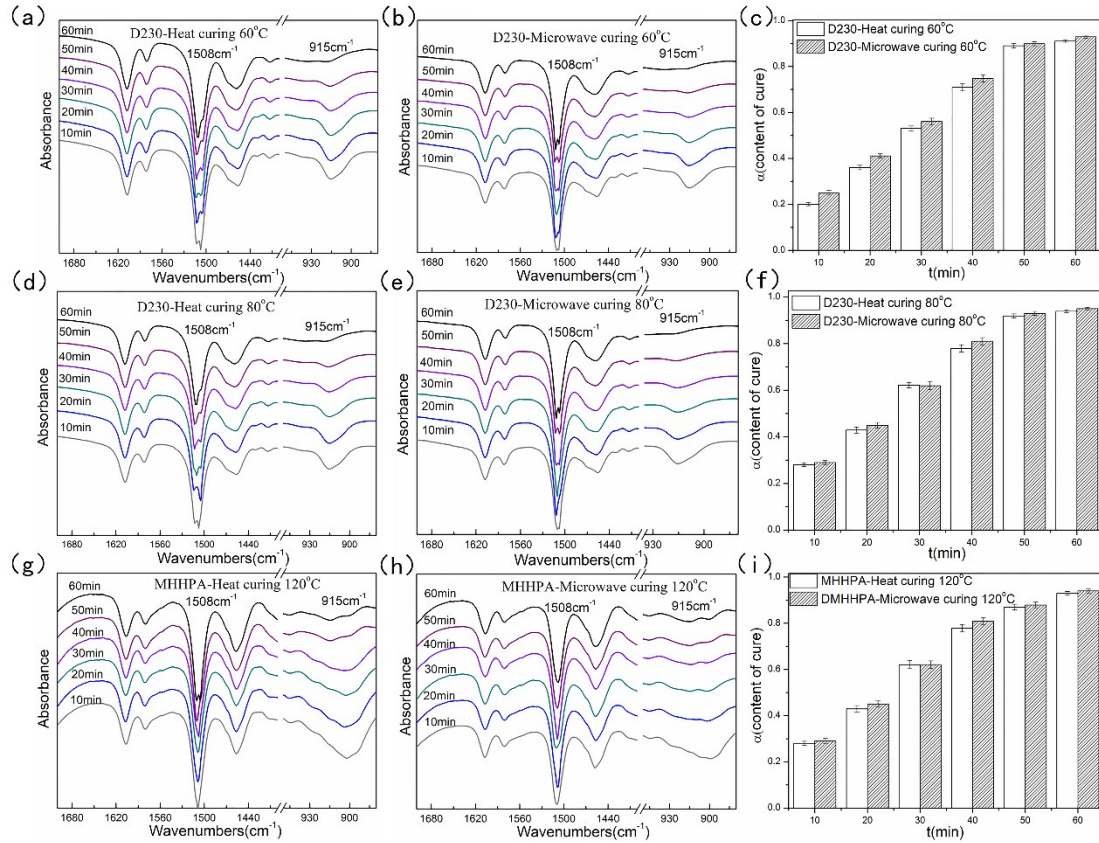
3 DSC was calibrated for each heating rate (Fig. S6).



5 **Fig. S6. Comparison of predicted Šesták - Berggren model rates with experimental Data. (a)-(d),**
6 **EP-D230; (e)-(f), EP-MHHPA.**

7 Data showed that the EP-D230 and EP-MHHPA system was in good accordance
8 with the experimental data, and Šesták - Berggren (m, n) model described the kinetics
9 of the curing reaction. A close match between the experimental data with predicted values
10 indicated the validity of the calculated kinetic parameters.

11



1

2 **Fig. S7.** Real-Time FTIR spectra and the corresponding conversion extent. (a), (b), (c): EP-D230
 3 curing at 60 °C; (d), (e), (f): EP-D230 curing at 80 °C; (g), (h), (i): EP-MHHPA curing at 120 °C.

4

5 **Table S5.** $lnt_{\alpha,i}$ values for the EP at 50-65 °C under heat and iso-thermal microwave irradiation.

α	0.1	0.2	0.3	0.4	0.5	0.6	0.7	0.8
$1/T_i, 1000$	$lnt_{\alpha,i}$ -heat							
3.09	-1.58	-2.15	-2.8	-3.35	-3.6	-4.2	-4.8	-5.4
3.05	-1.28	-1.8	-2.5	-3	-3.2	-3.9	-4.5	-5
3.00	-1.1	-1.5	-2.2	-2.7	-2.95	-3.7	-4.1	-4.6
2.96	-0.8	-1.2	-1.8	-2.4	-2.7	-3.2	-3.7	-4.4
	$lnt_{\alpha,i}$ -Microwave							
3.09	-2.1	-3.3	-4.6	-5.3	-6	-6.8	-7.4	-7.9
3.05	-1.69	-2.9	-4.1	-4.9	-5.7	-6.5	-7	-7.5
3.00	-1.63	-2.6	-3.9	-4.6	-5.3	-6.1	-6.7	-7.2
2.96	-1.17	-2.26	-3.5	-4.2	-4.9	-5.7	-6.3	-6.8

6

7 **Table S6.** $lnt_{\alpha,i}$ values for the EP at 70-85 °C under heat and iso-thermal microwave irradiation.

α	0.1	0.2	0.3	0.4	0.5	0.6	0.7	0.8
$1/T_i, 1000$	$lnt_{\alpha,i}$ -heat							

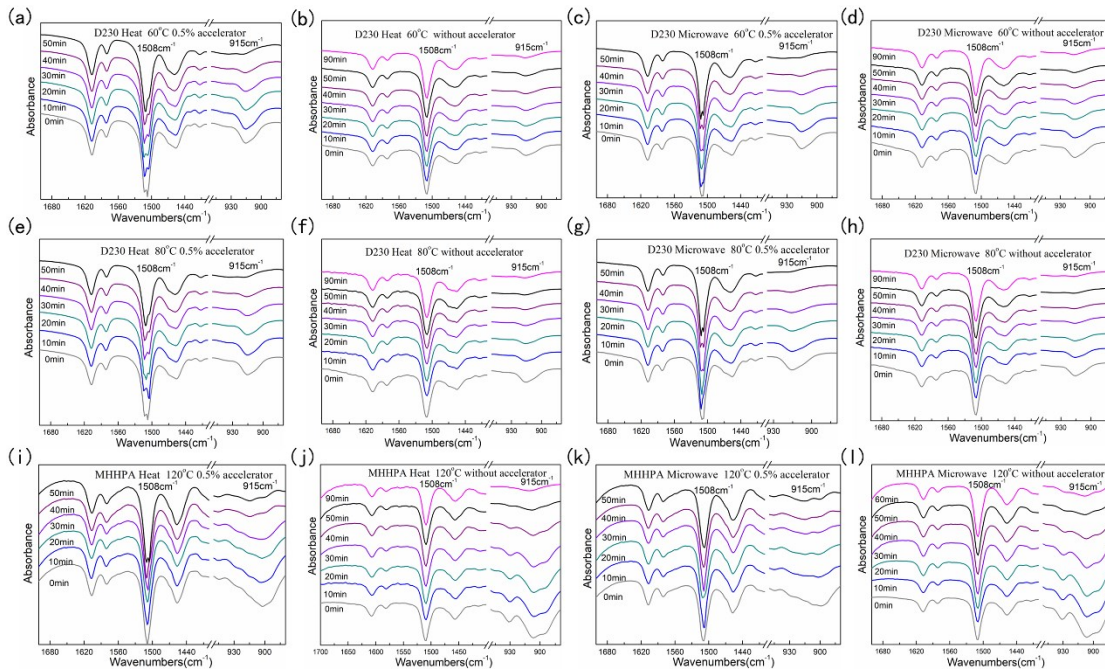
2.91	-1.82	-2.28	-2.46	-2.81	-3.08	-3.47	-3.71	-3.86
2.87	-1.66	-2.05	-2.31	-2.65	-2.88	-3.27	-3.55	-3.64
2.83	-1.48	-1.86	-2.15	-2.34	-2.56	-3.06	-3.28	-3.51
2.79	-1.22	-1.64	-1.89	-2.28	-2.46	-2.81	-3.18	-3.38
$lnt_{\alpha,i}$ -Microwave								
2.91	-1.75	-2.05	-2.34	-2.61	-3.01	-3.39	-3.65	-3.95
2.87	-1.46	-1.81	-2.11	-2.58	-2.81	-3.15	-3.41	-3.66
2.83	-1.26	-1.64	-1.94	-2.28	-2.66	-2.91	-3.24	-3.51
2.79	-1.19	-1.48	-1.72	-2.05	-2.44	-2.75	-3.01	-3.31

1

2 Table S7. $lnt_{\alpha,i}$ values for the EP at 110-125 °C under heat and iso-thermal microwave irradiation.

α	0.1	0.2	0.3	0.4	0.5	0.6	0.7	0.8
$1/T_i, 1000$	$lnt_{\alpha,i}$ -heat							
2.61	-1.97	-2.35	-2.66	-3.05	-3.08	-3.57	-3.94	-4.25
2.57	-1.76	-2.05	-2.31	-2.65	-2.88	-3.27	-3.55	-3.84
2.54	-1.48	-1.86	-2.15	-2.34	-2.56	-3.06	-3.28	-3.51
2.51	-1.22	-1.64	-1.89	-2.28	-2.46	-2.81	-3.18	-3.48
$lnt_{\alpha,i}$ -Microwave								
2.61	-1.9	-2.2	-2.44	-2.76	-3.16	-3.49	-3.75	-4.06
2.57	-1.66	-1.81	-2.11	-2.58	-2.81	-3.15	-3.41	-3.66
2.54	-1.26	-1.64	-1.94	-2.28	-2.66	-2.91	-3.24	-3.51
2.51	-1.19	-1.48	-1.72	-2.05	-2.44	-2.75	-3.01	-3.31

3



4

5 Fig. S8. Real-Time FTIR spectra of the resin with 0.5% and without accelerator.

1

2 References

- 3 1 Zhang. P.B, Shah. S.A.A, Gao. F, Sun. H, Cheng. J, Zhang. J.Y. Latent curing epoxy systems
4 with reduced curing temperature and improved stability. *Thermochim. Acta* 2019, 676, 130-
5 138.
- 6 2 Zvetkov. V.L, Ivanova. E.S, Calado. V. Comparative DSC kinetics of the reaction of
7 DGEBA with aromatic diamines IV. Iso-conversional kinetic analysis. *Thermochim. Acta*
8 2014, 596, 42-48.
- 9 3 Zvetkov. V.L, Djoumalisky. S, Ivanova. E.S. The non-isothermal DSC kinetics of
10 polyethylene terephthalate-epoxy compatible blends. *Thermochim. Acta* 2013, 553, 16-22.
- 11 4 Málek. J. The kinetic analysis of non-isothermal data. *Thermochim. Acta* 1992, 200, 257-
12 269.
- 13 5 Šimon P. Forty years of the Šesták-Berggren equation. *Thermochim. Acta* 2011, 520, 156-
14 157.
- 15 6 Vyazovkin. S, Burnham. A.K, Criado. J.M. Popescu. C. ICTAC Kinetics Committee
16 recommendations for performing kinetic computations on thermal analysis data.
17 *Thermochim. Acta* 2011, 520, 1-19.
- 18 7 Vergara. U.L, Sarrionandia. M, Gondra. K, Aurrekoetxea. J. Polymerization and curing
19 kinetics of furan resins under conventional and microwave heating. *Thermochim. Acta* 2014,
20 581, 92-99.
- 21 8 Vyazovkin. S, Wight. C.A. Model-free and model-fitting approaches to kinetic analysis of
22 isothermal and nonisothermal data. *Thermochim. Acta* 1999, 340-341, 53-68.
- 23 9 Javdanitehran. M, Berg. D.C, Duemichen. E, Ziegmann. G. An iterative approach for
24 isothermal curing kinetics modelling of an epoxy resin system. *Thermochim. Acta* 2016,
25 623, 72-79.
- 26 10 Mijovic. J, Fishbain. A, Wijaya. J. Mechanistic Modeling of Epoxy-Amine Kinetics. 2.
27 Comparison of Kinetics in Thermal and Microwave Fields. *Macromolecules*. 1992, 25, 986-
28 989.
- 29